Click to view poster presentation.

Permeability Prediction in Chalks*

Mohammad M. Alam[1], Ravi Sharma[2], Ida L. Fabricius[1], and Manika Prasad[2]

Search and Discovery Article #40506 (2010)
Posted February 8, 2010

*Adapted from extended abstract and poster presentation prepared for AAPG Annual Convention, Denver, Colorado, June 7-10, 2009

[1]Technical University of Denmark, Kgs. Lyngby, Denmark
[2]Colorado School of Mines, Golden, CO, USA (mprasad@mines.edu)

Summary

We investigated the use of velocity data to predict permeability from wireline logging data for the chalk reservoir in South Arne field, North Sea. We first examined the nature of relationships between permeability and porosity from core data and split these data in two ways: according to effective specific surface of grain volume, S_g, and according to hydraulic unit defined by Flow Zone Indicator (*FZI*). We then extended the porosity-permeability relationship to seismic velocity using laboratory data and applied them to well log data. We found that, S_g unit splitting works better for low permeable chalk while better *FZI* zoning is possible for high-permeable sedimentary rocks.

Introduction

Permeability determines the movement of hydrocarbon from a reservoir. Best possible permeability data could be achieved by laboratory measurement in core plugs. However, it is expensive, time consuming, and sometimes impossible to recover useable core material by drilling. Therefore, permeability is generally predicted from other physical properties of rocks. Permeability is classically described as a logarithmic function of porosity. However, several authors (Amaefule et al., 1993; Mortensen et al., 1998; Prasad, 2003; Fabricius et al., 2007) showed that, for same porosity rocks, permeability could vary in several orders of magnitude depending on type of rock, depositional environment, and diagenetic process. Kozeny (1927) described permeability as function of porosity and specific surface. Biot (1956a, b) showed theoretically that sound wave velocity in rocks depend on both porosity and permeability. Velocity is the primary data available for acquiring information about subsurface. Unfortunately, velocity-permeability relations are not well established. In contrast, velocity-porosity relations are well studied (e.g., Raymer et al., 1980; Nur et al., 1995). Prasad (2003) proposed velocity-permeability relations in sandstone according to hydraulic unit defined by *FZI*.

We studied velocity-permeability and velocity-porosity relations in terms of effective specific surface of grain volume, S_g units and *FZI* zones for North Sea chalk. The established relationships between velocity and permeability measured in core plug according to S_g unit and *FZI* zone

were used to predict permeability directly from velocity. Permeability was also predicted from porosity, calculated from velocity-porosity relationship for each S_g unit and *FZI* zone. Each method was tested for permeability prediction from well-log velocity data. Chalk from Ekofisk Formation of Paleogene age and from Tor Formation of Cretaceous age were investigated. These two formations are largely calcitic but have different silica and clay content. In general, the Ekofisk Formation has high specific surface area due to their high content (>12%) of silicate. The smaller specific surface area in the Tor formation is due to low content of silica and clay (<95%) (Fabricius et al., 2008).

Data

We used 12 core samples from SA-1 and Rigs-1 wells of South Arne field in central North Sea. Forty-four core data from Fabricius et al.(2008) were also used; it includes data from wells Rigs-1, Rigs-2 and SA-1. Compressional velocity data from wireline logs of SA-1 and Rigs-1 were used for permeability prediction. Predicted permeability was compared with core measured permeability achieved from GEUS (Geological Survey of Denmark and Greenland) CoreLab database. All core datasest include porosity, permeability as well as *Vp* and *Vs* under both saturated and dry condition.

Theory and methods

Based on laminar flow of fluid in porous media, Kozeny (1927) derived:

$$k = c\frac{\phi^3}{S^2} = c\frac{1}{S_g^2}\frac{\phi^3}{(1-\phi)^2} \qquad (1)$$

Where, k is liquid (Klinkenberg) permeability, φ is porosity and c is Kozeny's constant. S and S_g are grain surface per unit bulk and grain volume, respectively. Carman (1937) presented Kozeny's equation as:

$$k = \frac{1}{F_s\tau^2 S_g^2}\frac{\phi^3}{(1-\phi)^2} \qquad (2)$$

Where, F_s is a dimensionless shape factor and τ is tortuosity defined as the ratio between actual flow length, l_a and sample length, l. It can be seen that, $1/F_s\tau^2$ is the same as Kozeny's constant. However, it varies with the magnitude of difficulties of fluid flow associated with the internal structure of rocks and is fairly constant within the same hydraulic unit (Amaefule et al., 1993). Rearranging Equation 3, Amaefule et al. (1993) addressed the variability of Kozeny's constant as follows:

$$\left[0.0314\sqrt{\frac{k}{\phi}}\right] = \left[\frac{\phi}{(1-\phi)}\right]\left[\frac{1}{\sqrt{F_s}\tau S_g}\right] \qquad (3)$$

$$[RQI]=[\varepsilon]\,[FZI] \tag{4}$$

$$\log RQI = \log\varepsilon + \log FZI \tag{5}$$

Where, *RQI* is called Reservoir Quality Index, ε is the void ratio and *FZI* is described as Flow Zone Indicator. If permeability and *FZI* is expressed in mD and μm respectively:

$$\mathrm{FZI} = \frac{0.0314}{\varepsilon}\sqrt{\frac{k}{\phi}} \tag{6}$$

For homogeneous sediments like chalk, pores are likely to have high connectivity, so a concept of a torturous flow path is difficult in perceive. However, a part of the porosity might be ineffective to the flow due to a shielding effect, which could be described by a porosity dependent *c* factor of Kozeny's equation (Mortensen et al., 1998):

$$c = \left[4\cos\left\{\frac{1}{3}\arccos(2\phi-1)+\frac{4}{3}\pi\right\}+4\right] \tag{7}$$

Thus, introducing porosity dependent *c*, effective S_g becomes porosity independent and permeability variation could be separated according to S_g units. We used the term effective S_g, which is calculated from Equation 1, considering porosity dependent *c* (Equation 7). We converted the gas permeability (K_g) into Klinkenberg corrected (liquid) permeability by empirical relation for North Sea chalk (Mortensen et al., 1998):

$$k_k = 0.52k_g^{1.083} \tag{8}$$

Results and Discussion

The porosity-permeability relationship shows notable separation according to Ekofisk and Tor Formations (Figure 1a, b). From normal distribution of permeability, we defined three S_g units in Ekofisk Formation and one S_g unit in Tor formation (Figure 1b, c). Similarly, Two *FZI* zones in Ekofisk Formation and two *FZI* zones in Tor Formation were also assigned (Figure 1b, c). As expected, effective S_g units become porosity independent while *FZI* tends to increase with porosity (Figure 2).

From the variation of S_g and *FZI* with depth, stratigrapic units with respect to permeability could be identified (Figure 3). Not all S_g units and *FZI* zones are present in every well. This indicates spatial stratigraphic variation. In Rigs-1 and Rigs-2 there are two S_g units in Ekofisk Formation (ESG2 and ESG3), whereas SA-1 has only ESG1. *Sg* units do not show any variation in Tor formation. According to *FZI* zone, one additional stratigraphic zone (TFZI2) could be defined at the bottom of Tor Formation (Figure 3f).

We examined the relationship between compressional velocity and permeability according to the assigned S_g units and *FZI* zones for both dry and saturated condition (Figure 4). Within the assigned S_g units and *FZI* zones, significant correlations coefficient could be found in most cases. Established relationships were then applied to the same set of velocity data to predict permeability and compared with Klinkenberg permeability (Equation 8) (Figure 5). In a more traditional procedure porosity-V_p relationships were established according to the designated S_g units and *FZI* zones (Figure 6). Porosity calculated from these relationships was used for permeability calculation according to Equation 1 and Equation 6. Predicted permeability was then compared with the Klinkenberg permeability (Equation 8) (Figure 7). Figure 5 and Figure 7 show that predicted permeability according to S_g units and *FZI* zones is close to the measured permeability. Direct permeability prediction from V_p according to S_g units and *FZI* zones gives better result compared to prediction of porosity from velocity and then permeability from porosity. In both procedures predicted permeability by *FZI* zoning varies significantly from measured permeability below one milli-Darcy. In contrast, variation according to S_g unit is higher for permeability above one milli-Darcy. No significant difference was observed between prediction by using V_p-dry and V_p-sat. We repeated the above procedure for V_p-sat data achieved from wireline logging from well Rig-1 (Figure 8) and SA-1 (Figure 9). V_p-sat data suitably predict permeability in the assigned zones.

Conclusion

Distributing samples according to S_g units and *FZI* zones improves the permeability prediction. For low permeable (<1 mD) rocks, as North Sea chalk permeability variation for same porosity rock could be described well by separating into S_g unit. *FZI* zoning could give better result for high permeability (>1 mD) rocks.

Acknowledgements

The financial support from HTF (Højteknologifonden) is gratefully acknowledged. We thank DONG Energy for providing well log and core data.

References

Amaefule, J.O., M. Altunbay, D. Tiab, D.G. Kersey, and D.K. Keelan, 1993, Enhanced reservoir description: Using core and log data to identify hydraulic (flow) units and predict permeability in uncored intervals/wells: 68th Annual Technical Conference and Exhibition of the SPE: SPE Paper 26436. p. 1-16.

Biot, M.A., 1956a, Theory of propagation of elastic waves in a fluid-saturated porous solid. I. Low-frequency range: Journal of the Acoustic Society of America, v. 28, no. 2, p. 168-178.

Biot, M.A., 1956b, Theory of propagation of elastic waves in a fluid-saturated porous solid. II. Higher frequency range: Journal of the Acoustic Society of America, v 28, no. 2, p. 179-191.

Carman, P.C., 1937, Fluid flow through granular beds: Transactions IChemE, v. 15, p. S32-S44.

Fabricius, I.L., G. Baechle, G.P. Eberli, and R. Weger, 2007, Estimating permeability of carbonate rocks from porosity and v(p)/v(s): Geophysics, v. 72, no. 5, p. E185-E191.

Fabricius, I.L., L. Gommesen, A. Krogsbøll, and D. Olsen, 2008, Chalk porosity and sonic velocity versus burial depth: Influence of fluid pressure, hydrocarbons, and mineralogy: AAPG Bulletin, v. 92, no. 2, p. 201-223.

Mortensen, J., F. Engstrøm, and I. Lind, 1998, The relation among porosity, permeability, and specific surface of chalk from the Gorm field, Danish North Sea: SPE Reservoir Evaluation & Engineering, v. 1, no. 3, p. 245-251.

Gassmann, F., 1951, Elastic waves through a packing of spheres. Geophysics, v. 16, p. 673-685.

Kozeny, J., 1927, Ueber kapillare leitung des wassers im boden: Sitzungsberichte der Akademie der Wissenschaften in Wien, v. 136, 271-306.

Nur, A., G. Mavko, J. Dvorkin, and D. Gal, 1995, Critical porosity: The key to relating physical properties to porosity in rocks: 65th Annual International Meeting., SEG, Expanded Abstracts, p. 878-881.

Prasad, M., 2003, Velocity-permeability relations within hydraulic units: Geophysics, v. 68, no. 1, p. 108-117.

Raymer, D.S., E.R. Hunt, and J.S. Gardner, 1980, An improved sonic transit time-to-porosity transform: Presented at 21st Annual Meeting, SPWLA, paper P.

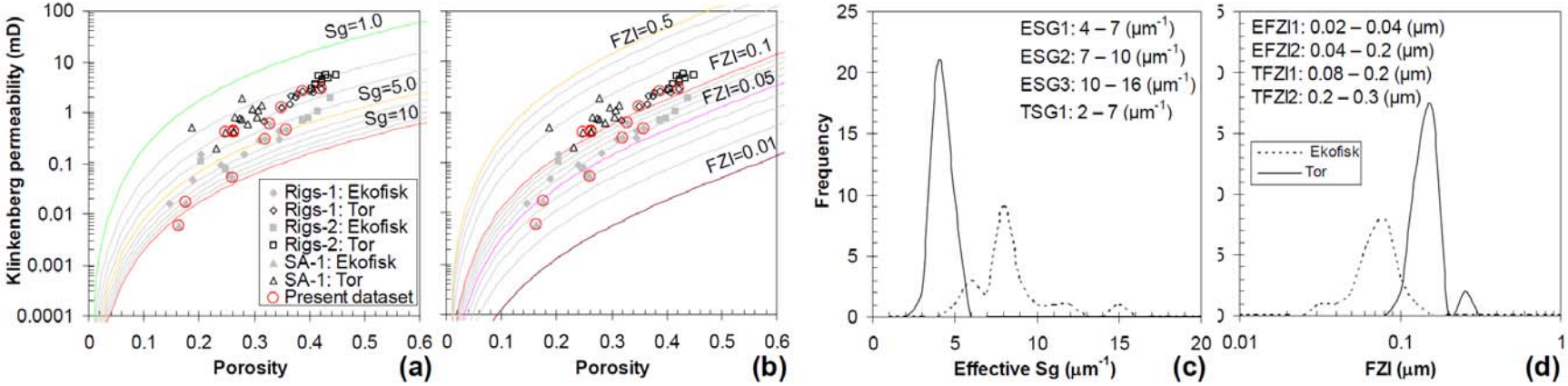

Figure 1. Theoretical and experimental relationship between porosity and permeability according to (a) S_g units and (b) *FZI* zones. Distribution of samples according to (c) S_g units and (d) *FZI* zones.

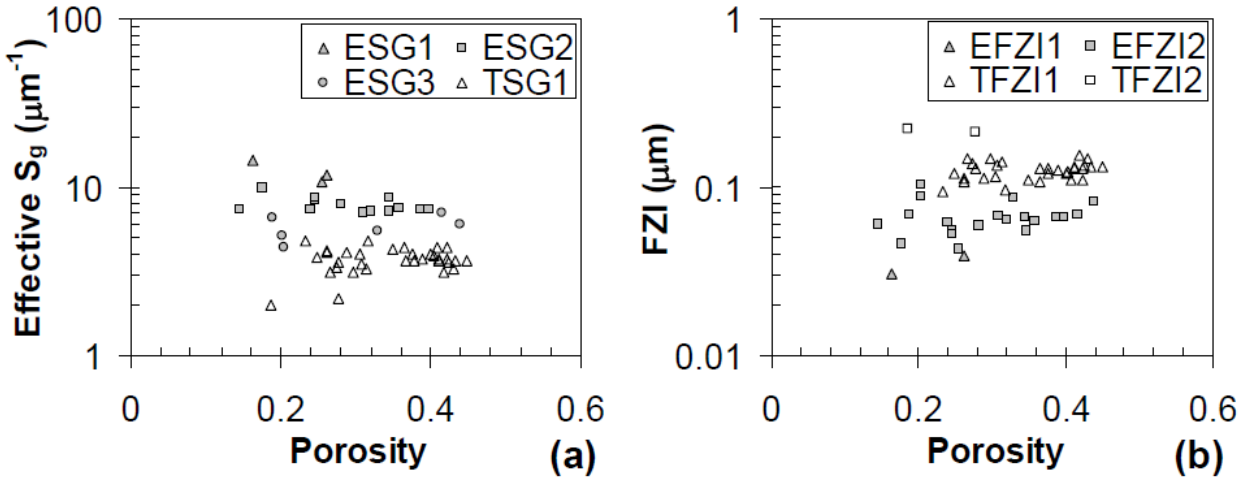

Figure 2. Relationship between porosity and (a) S_g units and (b) *FZI* zones.

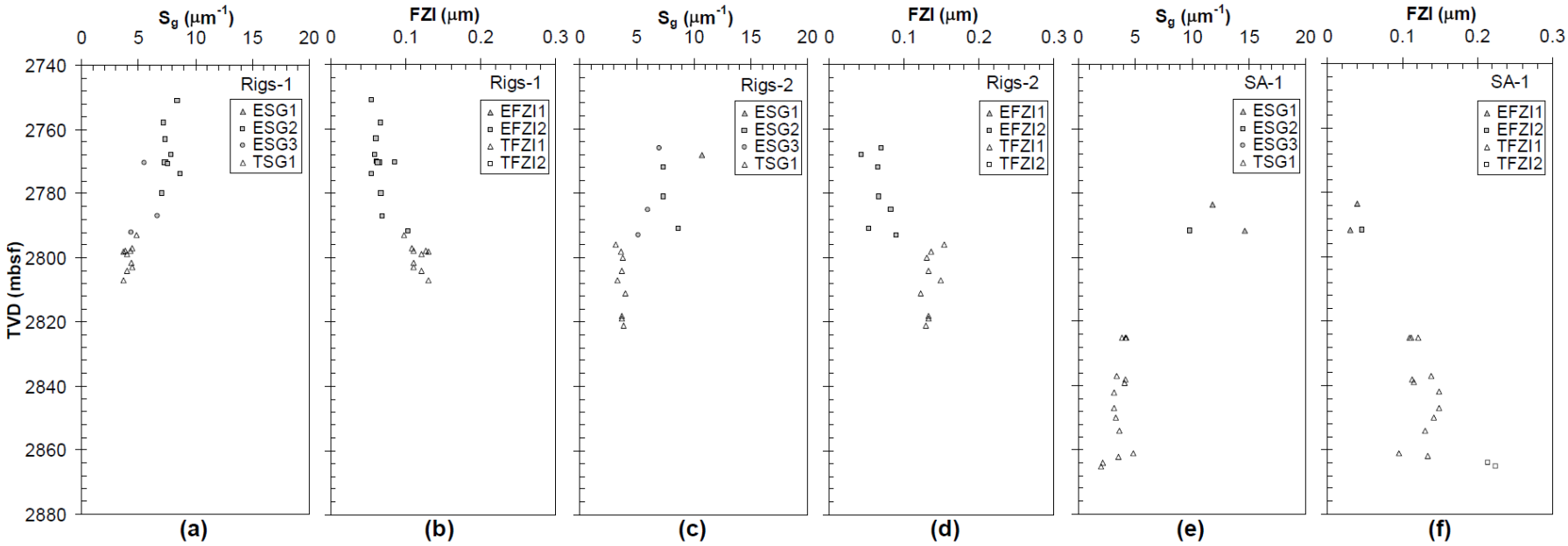

Figure 3. S_g units and *FZI* zones in the wells Rig-1, Rigs-2 and SA-1.

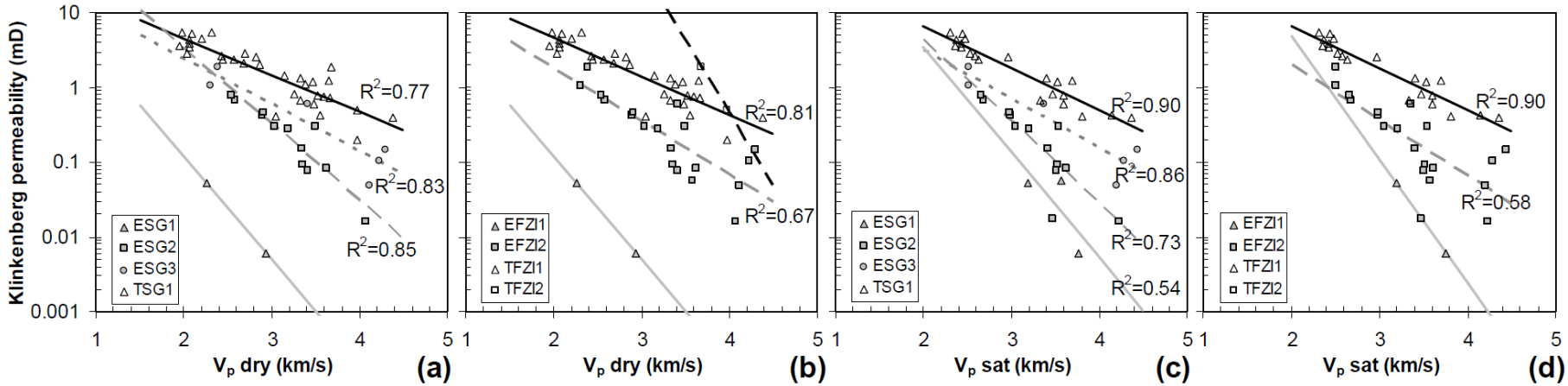

Figure 4. Compressional velocity-permeability relationships according to the designated S_g units and FZI zones. (a), (b) for dry data and (c), (d) for saturated data.

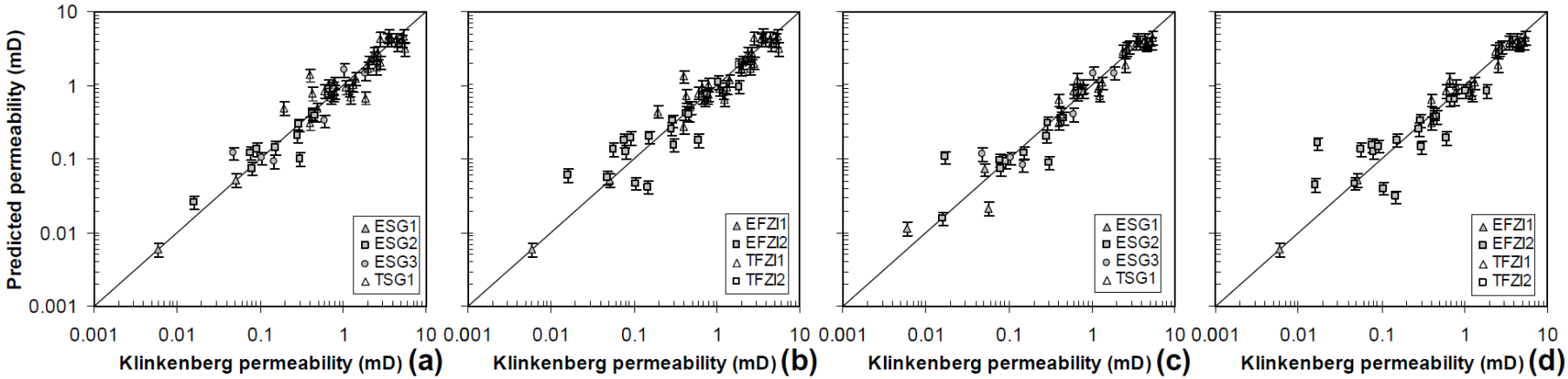

Figure 5. Comparison of permeability predicted directly from and Klinkenberg permeability (Equation 8) according to the designated S_g units and *FZI* zones. (a), (b) for dry data and (c), (d) for saturated data. Error bar shows 20% range.

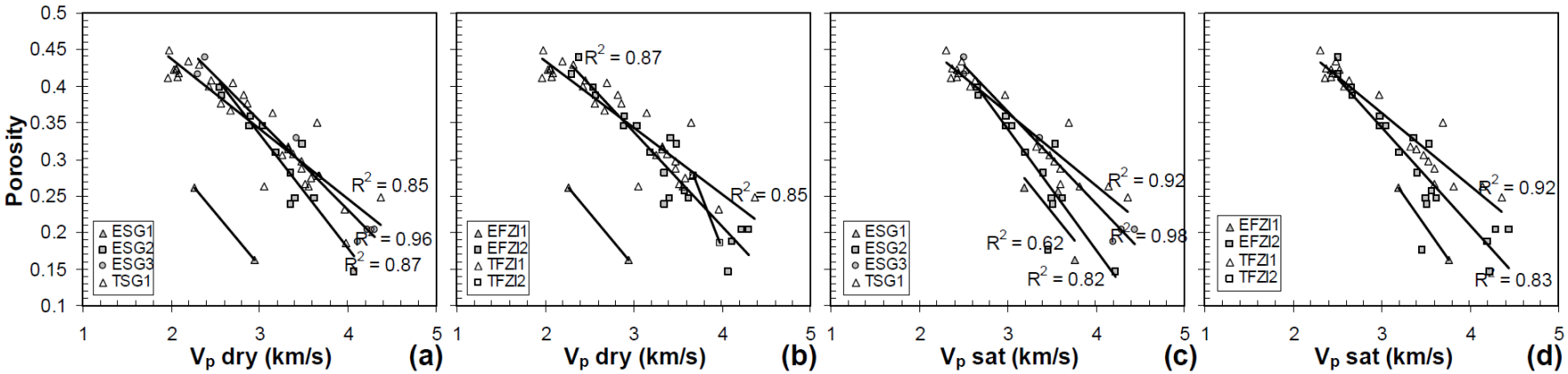

Figure 6. Compressional velocity-porosity relationships according to the designated S_g units and *FZI* zones. (a), (b) for dry data and (c), (d) for saturated data.

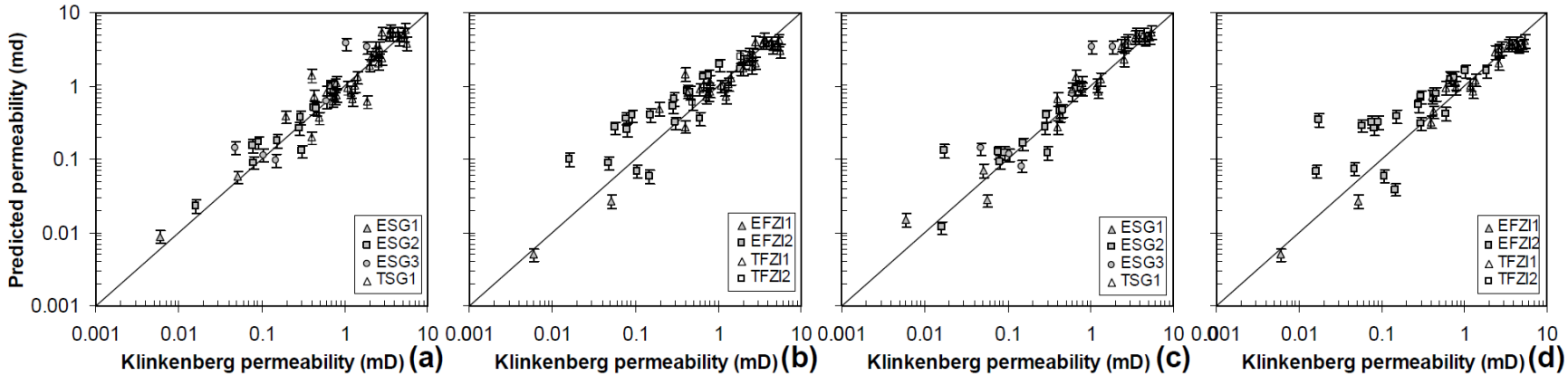

Figure 7. Comparison of permeability predicted from porosity (Equation 1 and 6) and Klinkenberg permeability (Equation 8) according to the designated S_g units and *FZI* zones. (a), (b) for dry data and (c), (d) for saturated data. Porosity was calculated from porosity-V_p relationship (Figure 5). Error bar shows 20% range.

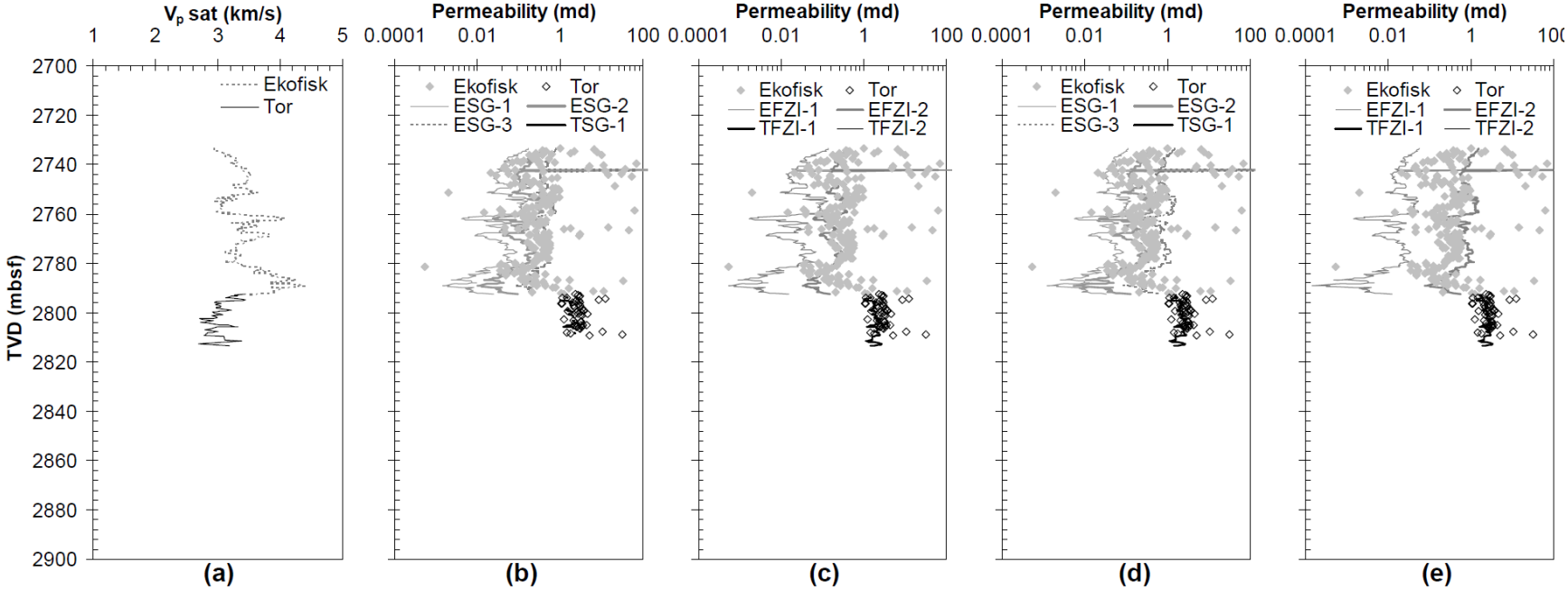

Figure 8. Predicted permeability for Rig-1 logging data. (a) V_p-sat (b), (c) Permeability estimated directly from V_p-sat for assigned S_g units and *FZI* zones. (d), (e) permeability predicted from porosity (Equation 1 and 6), calculated from porosity-V_p relationship.

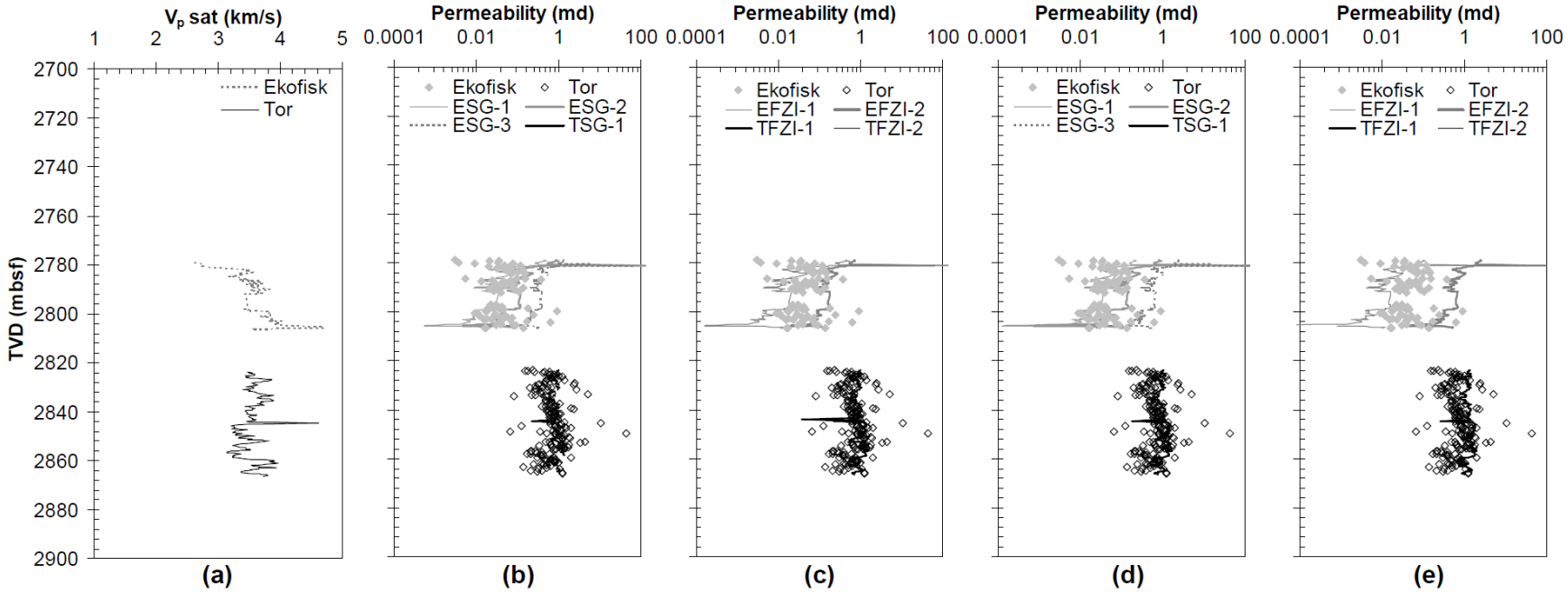

Figure 9. Predicted permeability for SA-1 logging data. (a) V_p-sat (b), (c) Permeability estimated directly from V_p-sat for assigned S_g units and *FZI* zones. (d), (e) permeability predicted from porosity (Equations 1 and 6), calculated from porosity-V_p relationship.